

OPTICAL CROSS-LINKS FOR MICROSATELLITE FLEETS*

Walter R. Leeb¹⁾, Andras Kalmar¹⁾, Klaus H. Kudielka¹⁾, Peter J. Winzer¹⁾, Bernhard Furch²⁾

¹⁾Vienna University of Technology, Institute of Communications and Radio Frequency Engineering, Vienna, Austria,

²⁾European Space Agency, Noordwijk, The Netherlands

ABSTRACT

In a study for the European Space Agency we explored architectures and terminal configurations for optical cross-links within fleets of microsatellites and assessed the applicability of available technologies. As an example we cover a scenario where four microsatellites form a planar, square formation of 1 km side length, where the data rate is 100 kbit/s, and where an active double-pass lidar between each of the satellites provides a ranging accuracy of better than 10 m. The terminals operate at a wavelength of 980 nm, the receive apertures have a diameter of 5 mm, and the size, mass, and prime power requirement of one terminal is estimated to be 60x80x70 mm³, 900 g, and 5 W, respectively.

INTRODUCTION

Fleets of satellites flying in close formation are presently investigated with the intention to break up the functions of large and complex spacecraft among several smaller, collaborating spacecraft. Such fleets (or "swarms") will require communication cross-links for which optical terminals represent a viable alternative to radio-frequency systems.

The concepts to be employed for optical communication links within microsatellite swarms will generally differ from those considered in the past for long-distance point-to-point free-space optical communication systems, the main reasons being drastically shorter link distances and lower data rates, even tighter limits on mass and size, and the required networking capability. This difference is especially visible in the area of pointing, acquisition and tracking, where much more simple solutions have to be found.

We establish the typical scenario of such a mission and give representative requirements. We then perform a basic comparison between optical and microwave systems and examine network topologies and access. Next we address the question of pointing, acquisition, and tracking. We assess technologies available for optical terminals, covering transmitters, receivers, beam shaping elements, and pointing methods. Design parameters both for optical communication and radar are traded off. We select an example scenario, design an optical communications/lidar terminal, and derive the terminal's performance characteristics. Our study shows that for specific swarm scenarios a communication network using miniature *optical* terminals based on state-of-the-art, commercially available opto-electronic components is not only a feasible but also an advantageous solution.

SATELLITE SWARM SCENARIO

Microsatellites may be characterized by a total mass of 10 to 100 kg. Several of them may operate in a fleet (swarm, cluster) to perform the function of a much larger, single satellite. Typical applications for a fleet of microsatellites ("µsat") are phased array telescopes (emulating a single telescope with low fill factor but with large baseline), interferometric missions asking for a large baseline to perform astronomic measurements, passive radiometry, and terrain mapping. With such applications in mind, low Earth orbits (LEOs) are presently of prime interest for µsats. For LEOs, one-dimensional, two-dimensional (i.e. planar), and three-dimensional configurations are feasible. The former would be a constellation resembling pearls on a string. Planar constellations await detailed investigations; it is believed that they would involve slightly different

* Copyright © 2002 by Walter Leeb. Published by the American Institute of Aeronautics and Astronautics, Inc. with permission

orbits, but still result in a configuration of (more or less) equal distance to the ground. The number of satellites forming a fleet could be limited by the wish to deploy all the fleet members by a single launch. To obtain first hand experience, a number of 3 to 5 is envisaged. Later, a fleet could consist of several ten μ sats.

The power available for optical terminals for communication and ranging is restricted to a fraction of the power available for the satellite payload and may be on the order of a few Watts. The presently envisaged data rates for intra-swarm links is anything from kbit/s to several 10 Mbit/s. This is somewhat in contrast to what is mentioned in a recent reference¹, where the authors conceive 250 Mbit/s links. The mutual distance may be in the range of 100 m to several km. In a free space link, not only communication between the μ sats but also the determination of distance and relative velocity (range, range rate) is not only feasible - by employing more or less the same hardware - but also highly desirable in order to assist formation keeping.

COMPARISON OF OPTICAL AND MICROWAVE SYSTEMS

To get a rough idea of how well optical communications is suited for a satellite fleet scenario with respect to microwave communications, we first compare two hypothetical systems by calculating their required transmit powers for an exemplary point-to-point link. The link parameters are those used for the optical system detailed later in the article, namely a distance $L = 1414$ m, a data rate $R = 100$ kbit/s, and an uncoded bit error probability $BEP_{ch} = 10^{-5}$.

For this comparison, we anticipate the following design parameters of the optical system: transmit antenna beam width of 6.5 degrees, receiver field of view of 5 degrees, sun-lit Earth atmosphere as background source. For a system operating at a wavelength of 980 nm employing NRZ format we will later derive a minimum optical input power at the receiver of -83 dBm. This in turn asks for an average transmit power of 19 dBm. The microwave link could operate at a wavelength of 13 cm (2.4 GHz band). With a typical system noise temperature of 200 K, a noise bandwidth equal to the data rate, and a signal-to-noise ratio of 13.5 dB (for phase shift keying), some -112 dBm are required at the receiver. We assume that, due to mass and volume constraints, only low-gain antennas with a gain of some 4 dB can be used. The required power at the microwave transmitter then amounts to approximately -17 dBm.

Thus, although the angular coverage of the microwave link is much higher than that of the optical link, the former requires 36 dB less power

at the transmit antenna! If we take into account that the "wall-plug efficiency" of microwave transmitters is up to one magnitude larger than that of lasers (or LEDs) the gap becomes even larger. On the other hand it could be argued that an optical transmit power of some 100 mW results in a DC power requirement of about one Watt, which not necessarily is a significant contributor to the satellite's power budget. (Note, however, that the number of transmitters per satellite is limited; the numbers given are for *one* crosslink only).

Even though the data rate from microsatellite to microsatellite might not exceed 100 kilobits per second, the aggregate data rate (sum of the data rates of all links operating simultaneously) may reach several hundred megabits per second. If maximum flexibility with respect to the satellite constellation is a concern, spatial decoupling of the individual links can definitely not be assumed for a microwave system. In such a case, the microsatellite network has to be designed with a shared channel in mind. Due to the much higher carrier frequency, the optical regime opens a virtually unlimited frequency band for data communications. For the present scenario, the bandwidth of a single optical channel is sufficient to accommodate the aggregate bandwidth expected. In the microwave regime it might be necessary to move to higher carrier frequencies, with little room for expansion.

For a rough estimate of mass and volume requirements, we assume that the expenses on power supply and baseband processing electronics are equal in both cases. Hence, we only compare the volume and mass requirements of the transceiver (opto-) electronics and of the antennas. Concerning transceiver electronics, a microwave transceiver (consisting of amplifiers, oscillators, mixers, etc.) certainly is more complex than an optical one (laser diode, photo receiver), but it has been demonstrated that complete microwave transceivers can be integrated on a single monolithic microwave integrated circuit (MMIC). We thus anticipate that, in both cases, a transceiver will consist of one or two packaged integrated circuits, the volume and mass of which will be approximately equal.

The configuration of the optical antenna subsystem (and thus its mass and volume) strongly depends on the required angular coverage. We anticipate that the mass of a single optical receive/transmit antenna (comprising a lens, an optical filter, diffractive optical elements, etc.) will not be significantly higher than that of a low-gain microwave antenna. If, on the other hand, multiple optical antennas or a pointing mechanism have to be used to cover the same field of view as a low-gain microwave antenna, the latter solution will definitely have a lower mass.

Of the above-mentioned performance criteria, mainly the large bandwidth available is a strong argument in favour of an optical communication/ranging system. Further arguments could be the high immunity with respect to electromagnetic interference (EMI) or with respect to interception. Another basic advantage when compared to an RF system would be the permissive availability of spectral bands.

OPTICAL NETWORK TOPOLOGY AND ACCESS

A satellite network may operate in the form of one of four basic topologies, just like a cabled data network: a mesh, a star, a ring, and a bus. The chosen topology has effect on network throughput, mean communication delays, necessity/complexity of routing algorithms, and also on ranging.

The physical communication channel of the satellite fleet must be shared by several communication links that have to operate independently and without interference. Like in a radio network, there are several methods to access the physical channel by the cluster satellites. Because of the narrow beamwidths achievable at optical frequencies, space division multiple access (SDMA) is especially attractive. However, if the complexity of the PAT system has to be kept low and the beamwidths used are large, the above condition can only be fulfilled for a small number of cluster members. SDMA communication links operate asynchronously and without the need for narrow optical filters. With time division multiple access (TDMA) all communication links occupy the same wavelength band and might also interfere spatially. The satellites transmit data sequentially in a bursty manner in the associated time slot. This type of multiple access requires time synchronization of all satellites in the cluster. Wavelength division multiple access (WDMA) systems ask for narrow optical filters with a wide field-of-view at the receiver and the necessity of maintaining a well defined, constant transmit wavelength at the transmitter. In a code division multiplex access (CDMA) system all satellites are allowed to transmit simultaneously, occupying the same wavelength band. Separation of the communication links is done by encoding each bit with the help of a spreading code. If coding and decoding is done in the electrical domain, the network is flexible and easily re-configurable. Recently, interest increased on implementations often called “optical (O-) CDMA” or “fiber-optic (FO-) CDMA”^{1,2,3} Optical CDMA is not yet a standard access method and hence its implementation is not yet state-of-the-art.

POINTING, ACQUISITION, AND TRACKING

Because of the small link distances and the low data rates in mind, optical terminals of μ sats can operate with relatively broad beamwidths. This allows to minimize the complexity and thus the mass and volume of the spatial pointing, acquisition and tracking system (PAT). Within a fleet of satellites a further simplification of the pointing problem may result if the satellite configuration is well defined (e.g. to be planar) and not subject to major reconfiguration. For the transmit antenna, these conditions would impose a welcome restriction on elevation angle. Concerning azimuth, using several TX antennas (or terminals) with sufficiently large beamwidths could result in a 360° coverage. To eliminate the need to point the optical receiver, a photo receiver with a large field-of-view should be used. We favor a system that will not need the capability of pointing and tracking optical beams but rather relies on proper orientation of the spacecraft involved and thus on wide-angle but fixed optical transmit and receive direction. In this case spatial acquisition will be reduced to simply switching-on the system and to a confirmation that a link is operable. Tracking is not required if the beamwidth is larger than - or on the order of - the angular uncertainty of the line of sight. Then passive pointing will suffice. Further, because of the large beamwidths and the constancy of relative terminal positions in a μ sat swarm, no point ahead will be required. Similarly, any Doppler effect will be negligible, not at least because we do not consider coherent reception. If pointing cannot be avoided, technologies promising low additional volume, mass, and power consumption have to be employed. Some suggestions in this direction are found later in this article.

TERMINAL CONCEPTS

We assume that transmit and receive apertures are designed as separate entities, due to their inherent smallness in the present application. In planar satellite constellations, optical terminals do not have to transmit radiation to (or receive radiation from) outside of the constellation plane. Hence, if a single terminal covers an angular range of 90° (azimuth) by 10° (elevation), a set of four such terminals, mounted on the microsatellite as shown in Fig. 1 (or, if space permits, at the top of a gravity gradient boom), already provides maximum connectivity. If a single light-emitting diode or laser diode is used as the optical source, some cylindrical beam shaping optics is required. If several (e.g. eight) sources with axially symmetric patterns are mounted side by side, but slightly tilted

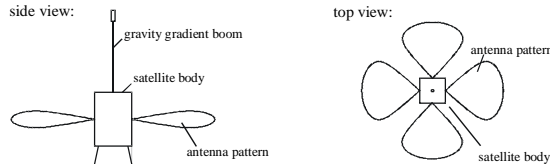


Fig. 1: Example of a radiation pattern attained by four terminals with fan-shaped transmit/receive characteristics, mounted on a microsatellite. Such a configuration is suitable for planar satellite formations.

with respect to each other, no additional optics is required to form the transmit beam. On the receive side, a single, large-area photo detector could be used in combination with a baffle covered by an optical filter. Alternatively, several baffled detectors may be arranged side by side, each one tilted by the field-of-view.

For completely re-configurable three-dimensional satellite constellations or for very large planar constellations (where beamwidths would have to be smaller than 10°), terminals may need some kind of pointing mechanism. Due to the small waists of the transmitted beams, miniature gimbaled mirrors implemented in MEMS (micro-electromechanical systems) technology are very attractive as pointing mechanisms in the transmit path. Besides being very compact, the MEMS mirror concept lends itself very well to an array design. If more than one crosslink is expected within the pointing mechanism's field-of-view, a multi-mirror device can be combined with a vertical-cavity surface-emitting laser (VCSEL) array and a microlens array (see Fig. 2). For the receive part of the terminals, we recommend against using pointing mechanisms for two reasons: First, significantly larger apertures (about 1 cm in diameter) than those for transmitting would have to be used, resulting in a significant contribution to the overall terminal mass. Second, acquisition sequences tend to be much more complicated if both the transmitter's and the receiver's field-of-view have to be scanned.

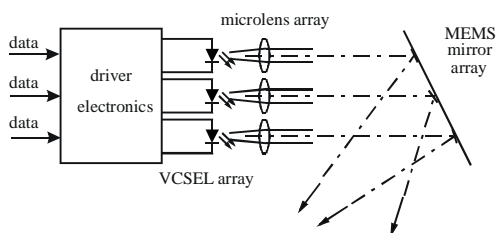


Fig. 2: Layout for a multi-beam transmitter for medium to narrow beam widths. MEMS mirrors are used for pointing.

TERMINAL TECHNOLOGIES

Because of the requirements on the terminals' compactness and ruggedness, we consider only semiconductor diodes as transmit sources. If the beam divergence is on the order of some 10° or larger and spectral quality and efficiency is not important, light emitting diodes (LEDs) based on GaAlAs with integrated cap lenses are the first choice. They allow for simple driving circuits and are available with output powers exceeding 100 mW. Conventional edge emitting laser diodes offer power conversion efficiencies exceeding 50% and output powers up to several Watts. In the wavelength range of 800 to 850 nm, maximum output powers of some 200 mW in a diffraction limited single transversal mode and with power conversion efficiencies of approximately 30% are available. If single mode operation is not an issue, a large number of general purpose laser diodes with up to one Watt output power from one diode are commercially available in the 800 nm range. Higher output powers (e.g. 3 W) require integrated arrays of partially coherent broad-area emitters. At 980 nm reliable, high power laser diodes for pumping Erbium-doped fiber amplifiers (EDFAs) are available. In the 1300 nm and 1550 nm wavelength ranges the maximum available power is significantly lower, i.e. some 50 mW. Vertical cavity surface emitting lasers (VCSELs) show low threshold currents and can be arranged in densely packed two-dimensional arrays. Commercially available VCSEL diodes reach output powers of a few mW in a single transversal mode at conversion efficiencies of 25%. They are available in the wavelength range from 750 nm to 1050 nm. Tunable and multi-wavelength lasers operating near $\lambda = 1550$ nm offer tuning ranges up to 60 nm. With integrated SOAs (semiconductor optical amplifiers), output powers of 10 mW are achievable, but the majority of the commercially available diodes reach just 1 mW.

As receiving element, the pin photo diode requires only a simple driving circuit and a low bias voltage. In applications where high background level dominates the overall signal-to-noise ratio or in receivers with optical preamplifiers (where signal-ASE beat noise dominates, ASE...amplified spontaneous emission), the noise contribution of the electrical preamplifier will be negligible. In other cases, an internal gain as provided by avalanche photodiodes (APDs) comes in handy, although accompanied by excess noise. As with pin photo diodes, silicon APDs can be used in the wavelength range of 300 nm to approximately 1050 nm. For 800 nm to 1700 nm, InGaAs diodes are available. Although we favor

systems not requiring active acquisition and tracking of the counter terminal, photo detectors usually employed as acquisition or tracking detectors may turn out advantageous if information about the relative angular position of the communicating satellites is desired. If a quadrant photodiode and some optics is employed instead of a single receive element, information about the receive beam's angle of arrival can be derived from the relative photo current generated by the four detector quadrants. Charge coupled devices (CCDs) and CMOS focal plane arrays could be considered as receive elements, too.⁴ Both are available in one-dimensional and two-dimensional configurations with up to a few thousand pixels in one dimension. The major drawback of this technology is the limited pixel readout frequency of some 10 MHz. Assuming a line sensor with 100 pixels and a pixel clock frequency of 10 MHz, a maximum data rate of 100 kbit/s and an angular resolution on the order of 1/100 of the field-of-view could be achieved. Another disadvantage is the large amount of readout electronics required (with its extra power consumption).

Using optical preamplification of the received signal may improve the performance of optical receivers, depending on the dominating noise term. Optical amplifiers are available as fiber amplifiers (e.g. in the form of EDFAs), as semiconductor optical amplifiers (SOAs), or in form of solid-state rod and slab amplifiers. In view of the tight mass and size limits applying to an optical μ sat terminal, mainly SOAs can be considered. However, they are usually designed for single transverse mode operation, which would mean that the receive antenna would effectively act in a diffraction-limited mode. A complex PAT system could be the consequence. On the other hand, SOAs with a multimode active region and equipped with multimode fibers may be beneficial, should such devices become available on the market.

To provide background suppression and channel selection (the latter in WDMA systems only), an optical bandpass filter has to be used at the receiver input. In general, wide field-of-view, narrow bandwidth, and low insertion loss are contrary requirements and a compromise will have to be found among them. Thin film interference filters are available with bandwidths down to 1 nm, their transmission varies from 60% for the narrow types to around 90% for filters with several 10 nm bandwidth. The center wavelength of a dielectric Fabry-Perot filter shifts with angle of incidence by some 1 to 2 nm/ $^\circ$, thus limiting the passband for wide-field-of-view applications. Due to their minimal angular dependence and low transmission loss, absorption filters based on GaAs are an attractive alternative to interference filters.

Undoped GaAs substrates effectively form a longpass filter with a cutoff wavelength of 920 nm. In combination with silicon photodiodes a bandpass characteristic of about 80 nm bandwidth can be achieved. Such an undoped GaAs absorption filter would require an operating wavelength around 980 nm.

If the uncertainty range of the counter terminal is only a few times the beam divergence or the field-of-view, switching between different transmit and receive apertures promises a simple solution to the pointing problem. In one implementation of a switched terminal, one of several transmit or receive apertures is activated, each with its own light source or detector. In this case switching and routing are performed in the electrical domain, resulting in high throughput and in redundancy. Switching may also be performed on antenna level in the optical domain, e.g. several transmit and/or receive apertures are connected to a single transmitter or receiver via fiber optic links using fiber optic switches. On the transmitter side, one could think of switching the optical output signal into different fibers whose bare ends acting as transmit antennas point into different directions. An approach in the form of a flat mirror tiltable along one or two axes in front of the terminal aperture is attractive due to the availability of lightweight electrostatically tiltable mirrors based on MEMS technology. This silicon-based technology allows to manufacture electrically driven mirrors with diameters between 300 and 2000 μ m with switching times as low as a few ms and angular movements between 3 $^\circ$ and 20 $^\circ$. (Such a system can, of course, also provide continuous pointing of narrow beams in two orthogonal directions.) Still another method would be to electro-mechanically swivel the output facet of a fiber which carries the transmit signal and acts as a transmit antenna (see Fig. 5). Two-axis gimbals carrying the optical terminal have been the choice for many of the optical lasercom terminals designed up to now. Although the gimbals available off the shelf are far too big and heavy for microsatellite applications, we do not know of any reason why this technology cannot also be extended to small terminals. Galvanometer actuators (small, but with permanent power consumption) or miniature dc motors or stepping motors (bigger, holding the position without drive power, with a resolution sufficient for μ sat application) could be employed as gimbal actuators.

SYSTEM PARAMETERS

Communications

The only two modulation formats that should seriously be considered for microsatellite swarms

are on-off keying (OOK), either implemented as return-to-zero (RZ) or as non return-to-zero (NRZ), and pulse position modulation (PPM). All three formats basically ask for the same receiver front-end^a, which – with reference to Fig. 3 – consists of a photo detector followed by low-noise amplification, filtering, and threshold decision.

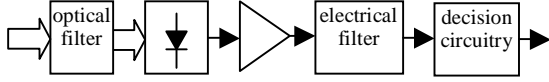


Fig. 3: Basic receiver frontend for RZ, NRZ, and PPM detection.

Expressions for the detected electrical signal and its associated noise in multiplying optical receiver structures subject to background radiation are given by

$$i = SMP, \quad (1)$$

where i denotes the mean photocurrent produced by the optical power P , S is the responsivity of the photodiode, and M stands for the avalanche gain, if an APD was employed as a detector. The photocurrent noise variance reads⁵

$$\sigma^2 = 2eSM^2PFB_e + 2eMI_dFB_e + 2eSM^2mN_bB_oFB_e + 4S^2M^2PN_bB_e + 2mS^2M^2N_b^2B_eB_o + N_{circuit}B_e, \quad (2)$$

with e being the electronic charge, F denoting the APD's noise figure, B_e standing for the electrical receiver bandwidth, I_d for the (multiplied) dark current, N_b for the background radiation power spectral density per mode, B_o for the optical filter bandwidth, m for the number of background modes intercepted by the receiver, and $N_{circuit}$ denotes the (thermal) circuit noise current density, which is basically given by the thermal noise current density ($N_{circuit} \approx 8kTC_D B_e$, $k...$ Boltzman's constant, $T...$ temperature, $C_D...$ capacitance of photodiode and preamplifier). The first and fourth term are *signal-dependent* and represent the signal shot noise and the signal-background beat noise, respectively. The *signal-independent* second, third, fifth, and sixth term represent the dark current shot noise, the background shot noise, the background-background beat noise, and the (thermal) noise of the electronic circuitry.

Depending on the modulation format and on whether the signal-dependent contribution of equ. (2) or the signal-independent part of equ. (2) is larger, different receiver design guidelines apply.

^a This is true if PPM is decoded by a slightly sub-optimum but much simpler threshold detection method instead of maximum-likelihood processing .

- For NRZ, the optimum receiver bandwidth will always have to be sought around 0.7 times the data rate R .
- For RZ and dominating signal-independent noise, the receiver bandwidth should be matched to the RZ pulse width to allow for best receiver performance. If d denotes the RZ duty cycle, matching the receiver bandwidth may result in a maximal RZ receiver sensitivity gain G of⁶

$$G_{RZ}[\text{dB}] \sim 5 \log(1/d) \quad [\text{dB}] \quad (3)$$

in terms of average received power over matched NRZ detection.

- For RZ and dominating signal-dependent noise, the optimum receiver bandwidth lies in the range of $0.7 R$, like in the NRZ case.
- For PPM, the receiver bandwidth always has to be matched to the signaling pulse width in order to determine the time slots of the received pulses. It can be shown that PPM with coding level C (requiring pulses of length $(C/2^C)T_{NRZ}$, where T_{NRZ} is the NRZ pulse duration) leads to a receiver sensitivity gain over NRZ of^b

$$G_{PPM}[\text{dB}] \sim 5 \log(C \cdot 2^{C-1}) \quad [\text{dB}]$$

for dominating signal-independent noise (4)

and of

$$G_{PPM}[\text{dB}] \sim 10 \log(C/2) \quad [\text{dB}]$$

for dominating signal-dependent noise. (5)

For low coding levels ($C \leq 2$) and dominating signal-dependent noise, PPM does not perform better than NRZ in terms of average power. The above sensitivity gain values only apply in terms of average power. If the transmitter is peak-power limited rather than average-power limited, all pulsed formats perform worse than NRZ.

Together with the received number of background modes the optical filter bandwidth sets the background noise level for the receiver. If the receiver field-of-view (FOV), Ω_{FOV} , is larger than the solid angle Ω_S subtended by the background source at the receiver, the number of background modes is given by⁵

$$m = \Omega_S A_{RX} / \lambda^2, \quad (6)$$

with A_{RX} being the receive aperture area and λ denoting the communication wavelength. Note that the number of background modes does *not* depend on the receiver's FOV in this case. This is in contrast to typical high-speed, long distance optical

^b In pulse position modulation, C bits - the "coding level" - are grouped to symbols prior transmission, leading to 2^C different symbols. Peak power P_{peak} and average power P_{av} are related via $P_{peak} = P_{av} \cdot 2^C$.

links, where the receiver's (diffraction-limited) FOV is typically much narrower than Ω_s . If extended sources (e.g. the Earth for satellite swarms in low-earth orbit (LEO)) are in the receiver's FOV, the formula

$$m = \Omega_{\text{FOV}} A_{\text{RX}} / \lambda^2 \quad (7)$$

applies.

Error correcting codes provide powerful means to reduce the required optical input power by several (2 to 8) dB, the exact value depending on the code, the channel bit error probability, and the decoding scheme. At the low data rates in mind, advanced decoding schemes (soft decoding) can be employed. Typically, for a channel bit error probability of $\text{BEP}_{\text{ch}} = 10^{-5}$, a decoded BEP_{dec} of better than 10^{-15} can be achieved.

For a direct-detection optical receiver, the average receive power required to obtain a certain BEP increases with data rate. If signal-independent noise dominates, the required power increases with the square-root of the data rate, while it increases linearly with data rate for dominating signal-dependent noise. Thus, if some total network throughput is specified, it makes sense to use continuous, low data rate communication rather than bursty communication. Buffering and appropriate routing within the swarm communication network could prove useful in converting bursts of data into continuous streams with lower power requirements at the transmitters.

Since complicated PAT subsystems have to be avoided in a typical microsatellite swarm scenario, a fairly broad transmit beam is required. Instead of specifying an antenna gain, as is done with high performance, diffraction-limited systems, it seems to be more appropriate to characterize the transmitter in terms of the horizontal and vertical transmit beam divergence angles α and β . We can then express the received power as

$$P_{\text{RX}} \propto P_{\text{TX}} / (\alpha\beta), \quad (8)$$

valid for $\alpha, \beta < \pi/2$. Going from the fan-shaped $10^\circ \times 90^\circ$ transmit beam shape of Fig. 1 to a pointing beam of size $6.5^\circ \times 6.5^\circ$ thus reduces the required transmit power by 13dB, although at the cost of some (switched) pointing.

In a free-space communication system, the link loss is proportional to L^2 (L...link distance). Reducing the link distance by a factor of two thus leads to a power gain of 6 dB. This important fact, which cannot be circumvented in conventional point-to-point links, can be made use of when designing the network topology and assigning physical channels. Depending on the actual swarm geometry, either a bus or a star topology could prove more advantageous by employing several short-distance links instead of a single long-

distance link. For a single link, the total received power is given by

$$P_{\text{RX}} \approx P_{\text{TX}} A_{\text{RX}} / (\alpha\beta L^2), \quad (9)$$

where A_{RX} stands for the receive aperture.

Radar

Single-pass radar systems^c are impractical due to the severe requirements on accurate time synchronisation within the swarm network. *Passive double-pass* radar relies on backscattering and hence would introduce unbearable high additional free-space loss. *Active double-pass radar* thus seems to be the best choice for a microsatellite swarm scenario. One can think of a situation where the target receives the radar-plus-communication signal, averages, introduces some fixed delay, and retransmits the signal.

A system primarily designed for communication is tailored to a minimum BEP_{ch} , requiring a particular signal-to-noise ratio (SNR) at the decision gate. Thus, the SNR dictated by communications is exactly the SNR available for radar^d. This leads to a ranging resolution of ⁷

$$\sigma_L > c \cdot d / [R \cdot (2 \text{SNR} \cdot n)^{1/2}], \quad (10)$$

for a double-pass radar system, where R denotes the data rate, d stands for the duty cycle, and n is the number of pulses the receiver averages over. (Here we assumed that RZ or PPM are employed for communications). According to equ. (10) high data rates lead to better radar performance because of the steeper pulse edges involved. However, higher data rates also need higher receive power to produce the same SNR – a tradeoff that has to be made when designing an actual system.

ILLUSTRATIVE DESIGN

Fleet scenario, communication requirements

To arrive at an illustrative design of an optical terminal we decided for a fleet of four satellites in low-Earth orbit (LEO), each of the satellites positioned at the corner of a square with a lateral length of $L' = 1000$ m (see Fig. 4). To first order, the satellites orbit in one and the same distance to the Earth surface, i.e. the formation is nominally planar. Within the plane, a slight distortion of the perfect square geometry towards a rhomb will be taken into account. To cover this and also some attitude uncertainties we will require an antenna

^c By single-pass radar we denote a radar system where the target itself is a radar receiver. On the other hand, we use the expression double-pass radar if the radar signal is reflected by the target and received at the location where it was transmitted.

^d For $\text{BEP}_{\text{ch}} = 10^{-5}$ we require $\text{SNR} = 12.6$ dB (dominating signal-dependent noise) and $\text{SNR} = 18.6$ dB (dominating signal-independent noise).

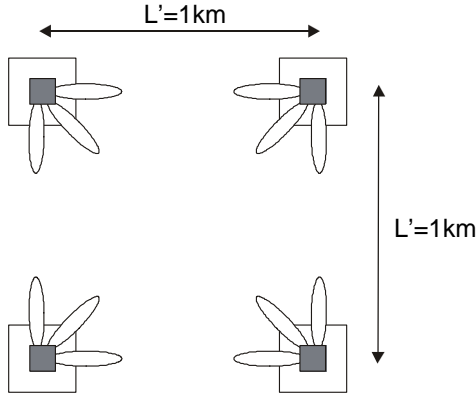


Fig. 4: Chosen satellite fleet configuration and terminal antenna pattern.

beamwidth of half-width divergence equal to or exceeding 2.5° .

Each satellite is equipped with one communication terminal. No continuous coarse pointing of the transmit and the receive antenna is implemented: For the transmit case, each terminal is able to serve three predefined directions that differ by 45° , i.e. coarse pointing is possible into one of three directions. For the receive case, three apertures acting as receive antennas are implemented; they illuminate one and the same photo detector. One way of realizing the antenna patterns discussed is sketched in Fig. 5. The full-width beam divergences in transmit case and receive case have been set to $\alpha_{TX} = 6.5^\circ$ and $\alpha_{FOV} = 5^\circ$. No fine pointing is required.

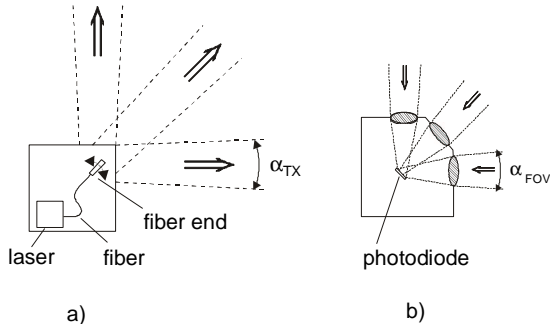


Fig. 5: Concept of transmitter (a) and receiver (b)

With the antenna pattern described, full mesh data transfer (and distance measurement) is possible. i.e. to each of the other satellites. Each terminal has only a single transmitter and a single receiver. On the other hand, in each terminal the transmitter and receiver operate independently and the transmit and the receive direction can be chosen independently. With this concept, several links can operate simultaneously. Figure 6 shows some of those possibilities. In case of Fig. 6a and Fig. 6c, full duplex data transmission is possible between two pairs of satellites. For these configurations,

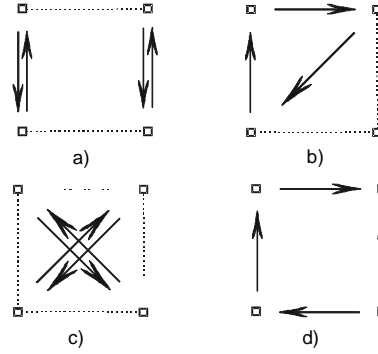


Fig. 6: Some of the possible simultaneous communication transfer configurations

active double-pass ranging can be performed as well. For the intra-swarm data rate we choose $R = 100$ kbit/s per link and direction. We will accept a channel bit error probability of $BEP_{ch} = 10^{-5}$. For the LEO orbit assumed, the receive antennas are directed tangentially to the orbit and hence will experience background radiation from the sun-lit Earth atmosphere. For the power spectral density of this extended source at a wavelength near $\lambda = 1\mu\text{m}$ we take a value of ⁸ $N_{Hz} = 3 \cdot 10^{-14} \text{ W}/(\text{Hz} \cdot \text{m}^2 \cdot \text{sr})$.

Choice terminal of technology and components

For the optical source, we decide for a laser diode with a wavelength somewhat below $\lambda = 1\mu\text{m}$. This will allow to use the most sensitive and compact photo detector available, namely a silicon APD. We further ask for a single-mode, fiber-coupled output interface. Then the simple coarse pointing scheme indicated in Fig. 5 can be implemented by just swiveling the fiber end. It also greatly simplifies the transmitter optics, as sketched in Fig. 7. At the envisaged wavelength a beam divergence of approximately $\alpha_{TX} = 6.5^\circ$ is achieved by employing a single-mode fiber for $1\mu\text{m}$.

For the optical source, we opt either for a laser developed for EDFA pumping ($\lambda = 980$ nm, 300 mW output power) or, with an eye towards low-noise detection, for a GaAlAs diode laser operating at $\lambda = 810$ nm (200 mW peak power into a single transverse free-space mode of elliptical cross-section, of which some 70 mW can be expected to

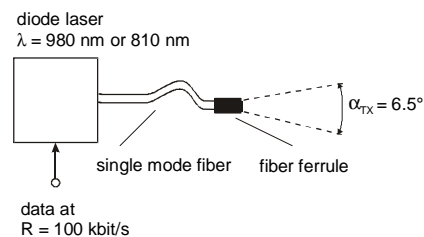


Fig. 7: Outline of the transmitter (one for each optical terminal)

be coupled into a single-mode fiber). For the modulation format we choose non-return-to-zero format (NRZ) as a baseline, but also consider a second option in the form of pulse position modulation (PPM). The latter format promises to operate with reduced average transmit power and also yields increased radar accuracy. We further suggest to implement forward error correcting coding, resulting in a coding gain of some 3 dB.

For the low data rates envisaged, a receiver based on a silicon APD will provide best sensitivity at the wavelength in question. We suggest to use one and the same diode for the three receive directions to be accommodated. For the two 45° -input directions the relationship between the detector diameter d_D , the receiver field-of-view α_{FOV} , and the focal length f of the optics is $d_D = \alpha_{FOV} \cdot f \cdot \sqrt{2}$. The resulting geometry for a single receive situation is sketched in Fig. 8. A dielectric coating carried by the focusing lens acts as an optical band pass filter.

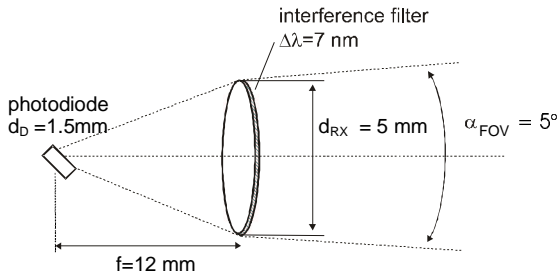


Fig. 8: Receiver geometry (single receive direction shown).

Performance characteristics

In addition to the system parameters already mentioned we assume 2 dB optics loss within the receiver, an electrical receiver bandwidth of 0.7 times the data rate in case of NRZ signaling, a link budget margin of 2 dB, and the possibility to average over $n = 1000$ pulses for radar purposes (see Table 1). Table 2 summarizes the calculated system performance for four cases, differing in wavelength (980 nm and 810 nm) and modulation scheme (NRZ and PPM with different coding level C). In all cases, the channel BEP is on the order of $\text{BEP}_{ch} = 10^{-5}$, and the decoded BEP is better than $\text{BEP}_{dec} = 10^{-17}$.

The sun-lit Earth atmosphere, as an extended background source, provides a total optical power of about -82 dBm at the detector. No other celestial body but the Sun would provide more background radiation. Regarding the optical filter bandwidth, the assumed 7 nm are no stringent requirement at 980 nm, since background shot noise is significantly below the dark current shot noise term at that wavelength. An optical bandwidth as large

Table 1: System parameters

data rate [bit/s]	R	100 000
wavelength [nm]	λ	980 or 810
transmitter divergence angle [deg]	α_{TX}	6.5
link distance [m]	L	1 414
background spectral radiance [W/(m ² Hz sr)]	N_{Hz}	3.00E-14
receiver aperture diameter [mm]	d_{RX}	5
receiver field-of-view [deg]	α_{FOV}	5
optics loss [dB]	L_O	2
optical bandwidth [nm]	$\Delta\lambda$	7
(primary) photo diode responsivity [A/W]	S	0.13 (@ 980 nm), 0.5 (@ 810 nm)
APD multiplication	M	100
APD noise figure	F	4
dark current [nA]	I_d	0.5
electrical NRZ bandwidth [Hz]	B_e	70 000
diode capacitance [pF]	C_d	10
(circuit noise current density) ^{1/2} [fA/sqrt(Hz)]	$\sqrt{N_{circuit}}$	54
link budget margin [dB]	L_M	2
radar: pulses to average	n	1 000

Table 2: System characteristics at two wavelengths and for two modulation formats

		980 nm NRZ	810 nm NRZ	980 nm PPM	810 nm PPM
transmitter peak power [mW]	$P_{TX,peak}$	160	50	320	50
average power @ TX [mW]	P_{TX}	80	25	20	13
coding level	C	-	-	4	2
link loss [dB]	L_L	90	90	90	90
peak signal power @ RX [dBm]	$P_{RX,peak}$	-72	-77	-69	-77
opt. background power [dBm]	P_b	-83	-81	-83	-81
average number of photons per bit		1 511	395	754	197
radar accuracy [m]	σ_L	9.4	8.9	2.9	6.3

as 80 nm would result only in a receiver sensitivity degradation of 1 dB. For $\lambda = 810 \text{ nm}$, the optical bandwidth for a 1 dB degradation is found to be 30 nm. The employed APD receiver has a sensitivity of 1511 photons/bit at 980 nm and 395 photons/bit at 810 nm for NRZ coding. The poor sensitivity at 980 nm is due to the low primary responsivity of 0.13 A/W at that wavelength. If near-infrared enhanced APDs with a dark current comparable to that assumed in Table 1 can be used,

the 980 nm receiver sensitivity can be expected to improve significantly. However, such devices seem not to be available presently.

Equations (3) to (5) indicated that a significant receiver sensitivity improvement in terms of average power requirements at the transmitter can be achieved by using either RZ or PPM. Since - taking NRZ as a baseline - we have some 3 dB to spend on peak laser power before reaching the technological limit of approximately 25 dBm at 980 nm, we could think of employing PPM with a coding level of 4 (or RZ with a duty cycle of about 40%). As a consequence, the use of RZ or PPM would lead to a reduction of the average required transmit power to 25% (PPM) or 74% (RZ) of the value required for NRZ. At 810 nm, only PPM with a coding level of 2 could be thought of, owing to the comparatively low power levels of state-of-the-art lasers at that wavelength. PPM with coding level 2 would lead to a 50% average power reduction. Since a good deal of the optical terminal's electrical power consumption will be assigned to the transmit laser, going to an impulsive coding format can thus significantly reduce the terminal's overall need for electrical energy.

Table 2 also shows that the ranging accuracy when averaging over 1000 pulses is on the order of a few meters. In some sense this poor radar performance is fundamental to the system, since the specified BEP_{ch} dictates the SNR and thus the ranging accuracy. However, as far as ranging is concerned, the use of PPM or RZ comes into its own: Assuming a pulse width of 5% of the bit duration^e, the ranging accuracy could be improved to some 0.5 m, even without the need for more pulses to average.

The size of the terminal will be given by that of the transmitter (TX), the receiver (RX), and supporting electronics. With an eye to Fig. 5 and the dimensions given in Fig. 8 we conjecture a size of 60x80x20 mm³ for each the TX and the RX. If we provide a volume of 60x80x50 mm³ for electronics we end up with a total size of 60x80x70 mm³. In the transmitter the contributions to the overall mass will be dominated by those for the laser and its cooling system, as well as for the swivel actuator. Together with the TX electronics this might sum up to 500 g. In the receiver, the lenses, the photo detector and associated electronics might sum up to 200 g. If we assign 200 g to the terminal housing the overall mass becomes 900 g. As for the power consumption, we assign 3 W to the - temperature-stabilized - laser, 0.5 W to the receiver frontend, and 1.5 W to

electronics. This gives a total power consumption of 5 W.

SUMMARY

Given the above scenario, a swarm communication network using miniature optical terminals seems feasible based on state-of-the-art, commercially available opto-electronic components, with a technologically-dictated emphasis on 980 nm. If some sort of pulsed coding is employed, the performance of an integrated optical radar subsystem is predicted to be accurate to better than 1m, representing a reasonable add-on to existing on-board GPS navigation.

ACKNOWLEDGEMENT

The contents of this paper evolved from a research project funded by the European Space Agency (Contract No. 14844/00). We also thank personnel from Surrey Satellite Technologies LTD/GB for valuable discussions.

REFERENCES

1. A. J. Mendez and R. M. Gagliardi, "Lasercom crosslinking for satellite clusters," Proc. SPIE, *Free Space Laser Communication Technologies XII*, vol. 4272, pp 50-59, 2001.
2. M. Azizoglu et al., "Optical CDMA via temporal codes," IEEE Trans. on Commun., 40, pp 1162-1170, July 1992.
3. S. W. Lee and D. H. Green, "Performance analysis of optical orthogonal codes in CDMA LANs," IEE Proc. Commun., 145, pp 265-271, August 1998.
4. L. J. Kozlowski et al., "Performance limits in visible and infrared image sensors," Techn. Digest of the 1999 IEEE Internat. Electron Devices Meeting, pp. 867-870, Dec. 1999.
5. W. R. Leeb, "Degradation of signal to noise ratio in optical free space data links due to background illumination", Applied Optics, 28, pp 3443-3449, 1989.
6. P. J. Winzer, A. Kalmar, "Sensitivity enhancement of optical receivers by impulsive coding," J. Lightwave Technol., 17 (2), 171-177, 1999.
7. M. I. Skolnik, Radar Handbook, McGraw-Hill, 1970.
8. W. K. Pratt, Laser Communication Systems, John Wiley, 1969.
9. A. J. Phillips, R. A. Cryan, J. M. Senior, "Novel laser intersatellite communication system employing optically preamplified PPM receivers," IEE Proc. Commun., 142 (1), 15-20, 1995.

^e Since the peak transmit power is technologically limited, such narrow (and thus high peak power) pulses can only be employed after changing other parameters of the scenario, e.g., by increasing the receive aperture size to 1 cm in case of a link distance reduced to 600 m.